

## Aesthetic Breast Surgery

# Histomorphologic Outcomes of GalaFLEX Scaffold Used in Breast Surgery: Clinical Follow-up From 6 Weeks to 63 Months

Bruce W. Van Natta, MD<sup>1</sup>; Catalina Pineda Molina, PhD<sup>2</sup>;  
Vincent Antonelli, MD; George S. Hussey, PhD;  
and Stephen F. Badylak, DVM, PhD, MD

Aesthetic Surgery Journal  
2025, Vol 00(0) 1–11  
Editorial Decision date: May 21, 2025; online  
publish-ahead-of-print July 4, 2025.  
© The Author(s) 2025. Published by Oxford  
University Press on behalf of The Aesthetic  
Society. All rights reserved. For commercial re-  
use, please contact [reprints@oup.com](mailto:reprints@oup.com) for  
reprints and translation rights for reprints. All other  
permissions can be obtained through our  
RightsLink service via the Permissions link on the  
article page on our site—for further information  
please contact [journals.permissions@oup.com](mailto:journals.permissions@oup.com).  
<https://doi.org/10.1093/asj/sjaf100>  
[www.aestheticsurgeryjournal.com](http://www.aestheticsurgeryjournal.com)

OXFORD  
UNIVERSITY PRESS

### Abstract

**Background:** The use of scaffolds in reconstructive and aesthetic breast surgeries for soft tissue reinforcement has increased over time. However, histomorphologic outcomes with the use of such materials are not typically reported. The present study describes the histologic findings associated with the use of the GalaFLEX Scaffold by BD (Franklin Lakes, NJ), an absorbable biosynthetic material, when used as soft tissue support in breast surgery.

**Objectives:** The present study evaluates the histomorphologic patterns of a 10-patient cohort that received GalaFLEX Scaffolds as soft tissue support in breast surgery, with and without breast implants.

**Methods:** Tissue biopsy specimens that included the implanted GalaFLEX Scaffold were collected during revision from 6 weeks to 63 months postimplantation. General staining and specific immunolabeling were used to determine cellular infiltration, tissue composition and organization, and vascularization.

**Results:** Biopsy specimens showed slow degradation of the GalaFLEX Scaffold, robust vascularization, mononuclear cell infiltration that decreased with time, and deposition of an organized collagenous connective tissue matrix in the interfiber space of the GalaFLEX Scaffold. There was no evidence for chronic inflammation or a foreign body response. The pattern of tissue remodeling around and within the fibers suggests a constructive tissue remodeling process rather than the formation of dense capsular tissue with contraction.

**Conclusions:** Implantation of the GalaFLEX Scaffold for reconstructive and cosmetic breast surgery appears to be safe and is associated with slow scaffold degradation, neovascularization, and mononuclear cell infiltration that diminishes with time, and a constructive remodeling response devoid of chronic inflammation or foreign body response. These conclusions are limited by the size of the 10-patient cohort.

### Level of Evidence: 4 (Therapeutic)

Reconstructive and aesthetic breast surgeries have significantly increased in popularity over the past 2 decades.<sup>1</sup> These procedures encompass a range of interventions, including aesthetic surgeries such as breast augmentation, mastopexy, reduction, correction of congenital deformities, revision surgeries, and reconstruction following cancer treatment.

Breast augmentation remains one of the most common aesthetic surgical procedures for women, with 2.2 million procedures performed globally in 2023—a 29% increase since 2021. Overall, the number of breast-related procedures performed by plastic surgeons exceeded 4.1 million in 2023.<sup>2</sup> In the United States alone, the American Society of Plastic Surgeons reported over 500,000 aesthetic breast procedures and more than 177,000 reconstructive surgeries in 2023.<sup>3</sup>

Breast reconstruction, which restores breast morphology following mastectomy or lumpectomy, has increasingly shifted toward implant-based techniques over flap-based methods.<sup>4</sup> Although not yet FDA approved for breast reconstruction applications, the use of scaffolds in

plastic and reconstructive breast surgeries has increased in recent years for a variety of reasons, including the ability to address surgical challenges of ptosis, thin skin flaps, reduced skin elasticity, and fluctuation in weight that can complicate breast reconstruction, among others.<sup>5,6</sup>

Dr Van Natta is an associate professor, Plastic Surgery Section, School of Medicine, Indiana University, Indianapolis, IN, USA; and is a clinical editor for *Aesthetic Surgery Journal*. Dr Pineda Molina is a research assistant professor, Dr Antonelli is a general surgery postdoctoral scholar, and Dr Badylak is a professor, Department of Surgery, School of Medicine, McGowan Institute for Regenerative Medicine, University of Pittsburgh, Pittsburgh, PA, USA. Dr Hussey is an assistant professor, Department of Pathology, School of Medicine, McGowan Institute for Regenerative Medicine, University of Pittsburgh, Pittsburgh, PA, USA.

#### Corresponding Author:

Dr Stephen F. Badylak, 450 Technology Drive, Suite 300, Pittsburgh, PA 15219, USA.  
E-mail: [badylaks@upmc.edu](mailto:badylaks@upmc.edu)

Biologic, biosynthetic, and synthetic scaffolds in breast surgeries are frequently used to reinforce soft tissue and/or provide implant coverage in various clinical scenarios, including mastopexy (with or without implants), prevent implant rotation and malposition, and correct symmastia and asymmetry following reconstructions.<sup>7,8</sup> Such scaffolds may enhance aesthetic outcomes by reshaping the implant pocket, offering improved support, and facilitating tissue integration.<sup>9</sup> Additionally, scaffolds have been shown to reduce the risk of implant-related complications, such as capsular contracture, a common issue in breast reconstruction.<sup>10</sup>

Since its introduction in 2011, the GalaFLEX Scaffold by Becton Dickinson &Co.—BD (Franklin Lakes, NJ) has emerged as an alternative to biologic and synthetic scaffolds derived from decellularized tissue extracellular matrices (ECM) or chemically derived polymers, respectively.<sup>7</sup> GalaFLEX is an absorbable knitted monofilament scaffold composed of poly-4-hydroxybutyrate (P4HB),<sup>11,12</sup> which degrades in the body to release its monomer 4-hydroxybutyrate (4HB), a molecule that is naturally present in mammalian tissue. Knitted P4HB meshes have previously been shown to be effective in abdominal wall reconstruction and tendon repair.<sup>12-14</sup> P4HB surgical meshes promote constructive tissue remodeling, reduce chronic inflammatory responses and fibrosis, and stimulate the secretion of antimicrobial peptides by macrophages.<sup>13-16</sup> Clinical applications of the GalaFLEX Scaffold in breast applications have shown its ability to provide mechanical strength during the wound healing process, which supports breast weight and maintains long-term tissue morphology, particularly when implanted in the lower pole of the breast.<sup>11</sup>

Previous studies have shown favorable outcomes with GalaFLEX Scaffold in a wide range of breast surgical procedures, including revision breast surgeries,<sup>5</sup> immediate<sup>17</sup> and 2-staged<sup>18</sup> prepectoral breast reconstruction, and direct-on-implant augmentative mastopexy.<sup>11,19</sup> However, few publications have reported the histomorphologic tissue integration outcomes of GalaFLEX breast implantation.<sup>11,20</sup> The present study evaluated the histopathologic characteristics and tissue integration patterns of GalaFLEX Scaffolds used as soft tissue support in breast tissue from a 10-patient cohort, with implantation times ranging from 6 weeks to 63 months.

## METHODS

The present study has been reviewed by Pearl IRB. An exemption was granted on the research project according to federal regulations: 45 CFR 46.104(d)(4) Secondary Research Uses of Data or Specimens 45 CFR 46.104(d)(4)(ii), 45 CFR 46.104(d)(4)(iii).

## Surgical Procedures

The present study includes the histologic description of breast biopsy specimens from 10 patients that received a GalaFLEX Scaffold implant as part of their elective surgical plan. The primary surgical procedures included mastopexies, reductions, and implant augmentations as described in Table 1. Surgeries were performed between 2013 and 2016. All patients had informed consent for the primary procedure. The primary reason for revision in each patient was unrelated to the implanted scaffold. All primary surgical procedures and revisions were performed by a single plastic and reconstructive surgeon.

## Specimen Collection

Tissue biopsy specimens were collected during revision surgeries performed between 2013 and 2020, ranging from 6 weeks to 63 months post-implantation. In all cases, samples were collected from

**Table 1.** Patient Histories of GalaFLEX Explant Specimens Evaluated in This Report

Patient number	Original surgery	Explant timepoint	Breast implant?	Reason for revision surgery
1	Dual plane augmentation with mastopexy	6 Weeks	Yes	Persistent ptosis
2	Mastopexy	6 Months	No	Recurrent ptosis
3	Mastopexy	7 Months	No	Weight loss post bariatric
4	Reduction	9 Months	No	Implant augmentation
5	Augmentation with inframammary skin excision	11 Months	Yes	Persistent ptosis
6	Mastopexy	24 Months	No	Macromastia
7	Augmentation	27 Months	Yes	Correction of implant malposition
8	Reduction	30 Months	No	Recurrent macromastia
9	Mastopexy	52 Months	No	Scar revision
10	Reduction	63 Months	No	Recurrent macromastia

waste tissue. From each patient, 1 to 3 samples containing the GalaFLEX Scaffold and surrounding breast tissue were harvested and placed in 10% neutral buffered formalin followed by washes and preservation in 70% to -95% ethanol.

## Histomorphologic and Immunolabeling Methods

Fixed specimens were further processed at Alizée Pathology, LLC (Thurmont, MD). Each tissue sample was embedded in paraffin, sectioned, and stained with hematoxylin & eosin (H&E) and Masson's trichrome (MT). Each sample was separately immunolabeled against CD-31 (Cat. No. PS5-16301, polyclonal rabbit) Invitrogen (Waltham, MA), smooth muscle actin (SMA) (Cat. No. BSB 5034, monoclonal mouse) BioSB (Goleta, CA), collagen Type I (Cat. No. ab138492, monoclonal rabbit) Abcam (Waltham, MA), and collagen Type III (Cat. No. ab7778, polyclonal rabbit) Abcam. Briefly, each slide was deparaffinized with xylene and rehydrated with sequential washes in decreasing concentrations of ethanol. Following an antigen retrieval process, the slide was incubated with the primary antibody. Indirect detection of the antigen-antibody complex was performed with one of the following secondary antibodies: Rabbit-on-Farma HRP (Cat No. BRR4009) Biocare Medical (Houston, TX) or Mouse-on-Farma HRP (Cat No. BRR4002) Biocare Medical, and visualized with DAB (Cat No. ACT500) ScTek Laboratories (Logan, UT). Finally, each slide was counterstained with hematoxylin. The presence and morphology of the P4HB fibers and the tissue response to the implanted GalaFLEX Scaffold were evaluated for cellular infiltration, tissue composition and organization, and vascularization. Two independent pathologists, 1 at Alizée Pathology and 1 at the McGowan Institute for Regenerative Medicine, provided a qualitative analysis of the samples.

**Table 2.** Demographic Data From Patients

Patient number	Age (years)	Height	Weight (pounds)	BMI	BMI category <sup>a</sup>	Parity	Breastfed
1	33	5'5"	115	19.1	Healthy weight	G2P2	Yes
2	35	5'8"	138	21.0	Healthy weight	G3P4	Yes
3	50	5'0"	120	23.4	Healthy weight	G2P2	Unknown
4	62	5'1"	103	19.5	Healthy weight	G2P2	Yes
5	40	5'2"	128	23.4	Healthy weight	G7P3	Yes
6	53	5'6"	135	21.8	Healthy weight	G2P3	Yes
7	49	5'4"	120	20.6	Healthy weight	G2P2	Yes
8	48	5'4"	120	20.6	Healthy weight	G2P2	Yes
9	64	5'4"	165	28.3	Overweight	G2P2	Yes
10	58	5'6"	145	23.4	Healthy weight	G2P2	No

<sup>a</sup>CDC's BMI categories: Underweight (BMI < 18.5), healthy weight (BMI 18.5-24.9), overweight (BMI 25-39.9), and obese (BMI ≥40).<sup>21</sup>

## RESULTS

### Patient Demographics

Samples from 10 female patients were included in this study. All patients were in good health at the time of primary and revision surgeries. The age of the patients at the time of the primary surgery ranged between 30 and 64 years old. The BMI for 9 patients ranged within a healthy weight category, and 1 patient was categorized as overweight, based on the BMI metrics defined by the Centers for Disease Control and Prevention (CDC).<sup>21</sup> All patients had previously had pregnancies, with 8 of these patients confirmed to have breastfed. A summary of demographic information from the patients is presented in Table 2.

Gross inspection of the implanted GalaFLEX scaffolds at the time of revision surgery showed good tissue integration and good vascularization in all cases. None of the patients showed signs of infection or inflammation at the implant site. For all patients, revision surgeries included the removal of a section of tissue as part of the procedure, which contained GalaFLEX scaffold.

### GalaFLEX Scaffold Material Was Visible in Breast Tissue From All Samples Ranging From 6 Weeks to 63 Months Post-implantation

All explanted specimens showed the presence of the P4HB fibers or residual P4HB material surrounded by various numbers of cells and vascularized ECM. These fibers did not stain positively with H&E (Figure 1). However, the fibers were visible as "gray" colored material in MT-stained sections (Figure 2). The GalaFLEX Scaffold fibers were clearly identifiable within round to oval clear spaces early in the series, with the empty spaces becoming more irregular in shape and size at later time points, and the gray fibers becoming fragmented and less abundant. The fibers had well-defined surfaces, with acellular and homogeneous staining that varied with the duration of the implant.

For all specimens at the earlier timepoints (6 weeks and 6-11 months) there was no appreciable degradation and no visible fragmentation of the fibers. As the length of time of implantation progressed (24-63 months), the integrity of the fibers diminished as evidenced by fragmentation of the material and more frequent "folding" that results

from the microtome knife as the thin, 5 to 7  $\mu$ M sections are created (Figure 1). In addition, the gray color intensity of the material diminishes with time. Moreover, the total area within the fiber spaces that was occupied by the P4HB material typically diminished compared with the area that was occupied by the material at the earlier time points. As shown in samples at 27, 30, 52, and 63 months, these areas were occupied with new ECM deposited around the fibers.

### GalaFLEX Scaffolds Promote a Constructive Host Tissue Response

Evaluation of the specimens at all timepoints showed a non-adverse host tissue integration around and within the GalaFLEX Scaffold, with no signs of tissue encapsulation or foreign body response. The cellular infiltrate present in these samples was dominated by mononuclear cells that had morphology consistent with macrophages with lesser number of fibroblasts. The quantity of these cells within the tissue specimens diminished with time. The earliest specimen, at 6 weeks, showed the greatest number of mononuclear cells and these cells tended to be arranged in clusters. By the 6 to 11-month timepoints, the number and distribution of cells appeared to reach a steady state; that is, although cells undoubtedly continuously migrate into the scaffold, the number and distribution of these cells are not consistent with a typical inflammatory response but rather a healthy tissue remodeling process. Specifically, there was a virtual absence of polymorphonuclear cells and foci of necrosis and multinucleate giant cells, and there was a modest decrease in vascularization. The distribution of the mononuclear cells can be found both adjacent to and between the fibers of the GalaFLEX Scaffold. One of the more notable findings was the mononuclear cell distribution at later timepoints. Specifically, these cells were not concentrated adjacent to the GalaFLEX fibers as is typically seen with synthetic surgical meshes (Figure 1). Rather, these cells were present either individually or in small clusters in the interfiber space. In addition, there were rare multinucleate giant cells present in the earlier samples (6 weeks and 6 months) and such cells were virtually absent from the later time point specimens. The multinucleate giant cell is the *sine qua non* of the foreign body response; thus, this classic tissue response to biomaterials that reside for longer periods of time in the body does not apply herein.

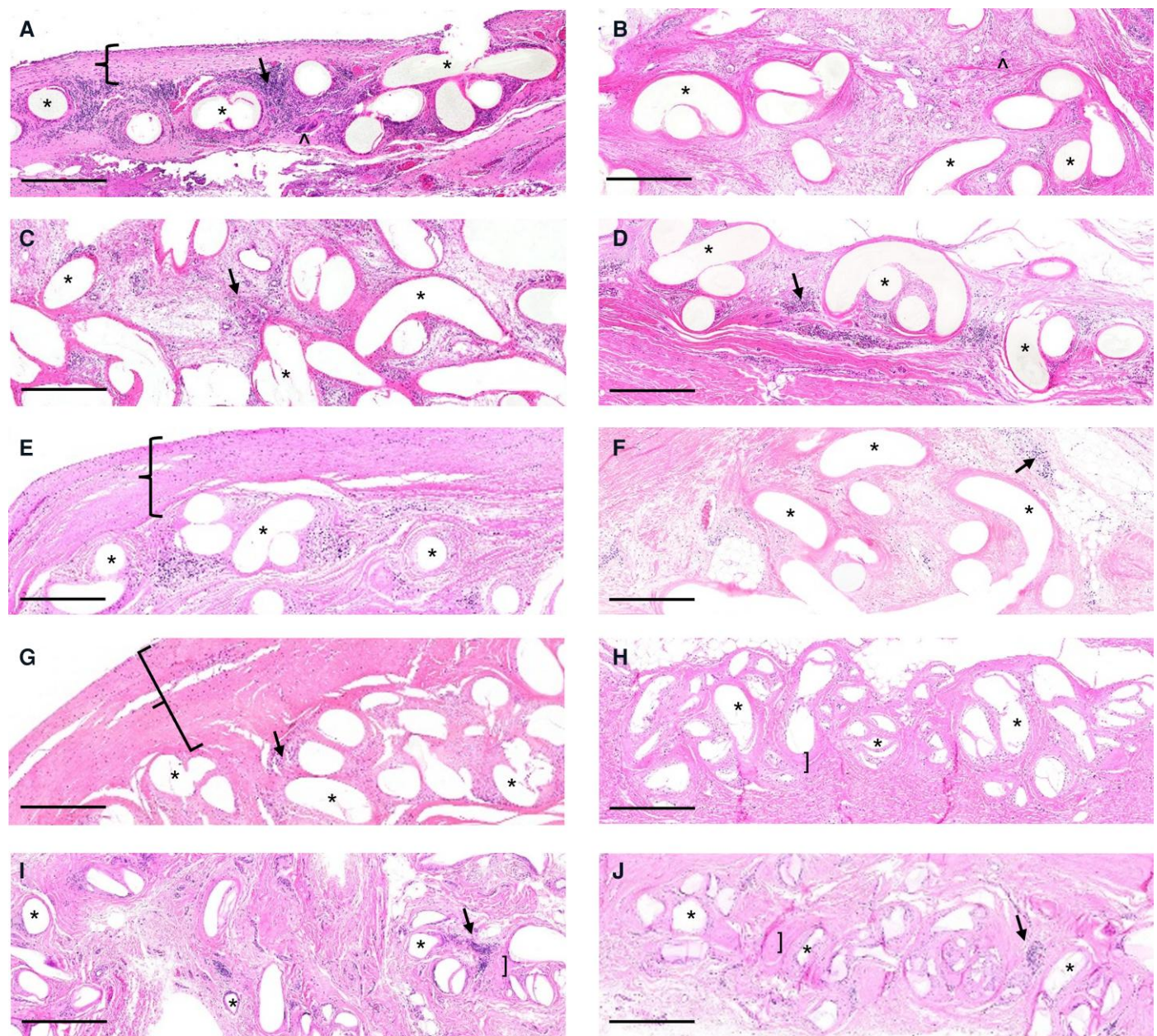


**Figure 1.** Cellular response to GalaFLEX Scaffolds in the breast tissue. Representative images of hematoxylin and eosin stained cross sections at 6 weeks (A), 6 months (B), 7 months (C), 9 months (D), 11 months (E), 24 months (F), 27 months (G), 30 months (H), 52 months (I), and 63 months (J) after GalaFLEX Scaffold implantation in the breast. Scale bars 500  $\mu$ m. Asterisks (\*) identify the poly-4-hydroxybutyrate (P4HB) fiber or P4HB remnant material location within the tissue. Right bracket (]) indicate new tissue deposition in areas previously occupied by P4HB fibers. Arrows (→) identify the infiltration of mononuclear cells. Arrowheads (^) show the presence of multinucleate giant cells. Left braces ({})) indicate an organized band of connective tissue immediately adjacent to the silicone implant location.

The other cells that were present as part of the infiltrate and remodeling tissue include the endothelial cells that compose the vasculature and the fibroblasts that contribute to the collagen-rich ECM. These cells are further described in the following sections.

## GalaFLEX Scaffold Does Not Promote Capsular Contraction in the Human Breast Tissue

Collagenous connective tissue was present in and around all P4HB fibers within these specimens. This connective tissue filled the entire interfiber space and was associated with the presence of spindle-shaped cells consistent with fibroblasts. Fibroblasts secrete the collagenous ECM.<sup>22,23</sup> The confirmation that these specimens were dominated by

collagen can be found in MT-stained slides (Figure 2) and the immunolabeled slides for collagen Types I (Figure 3) and III (Figure 4).

The deposition of the collagenous fibrous tissue occurred relatively early following implantation and appears as swarming bundles between the P4HB fibers. The earliest timepoint examined in this study was 6 weeks post-implantation, at which time the collagenous connective tissue was less organized (more randomly oriented). The second earliest timepoint examined in this study was 6 months and the connective tissue was more dense and less randomly organized compared with the 6-week timepoint, often present in aligned bundles traversing the interfiber space. By the 11-month time point, there was evidence of progressive connective tissue remodeling, and the eventual consistent presence of organized collagenous connective tissue arranged in linear bands and swarming bundles surrounding the embedded P4HB

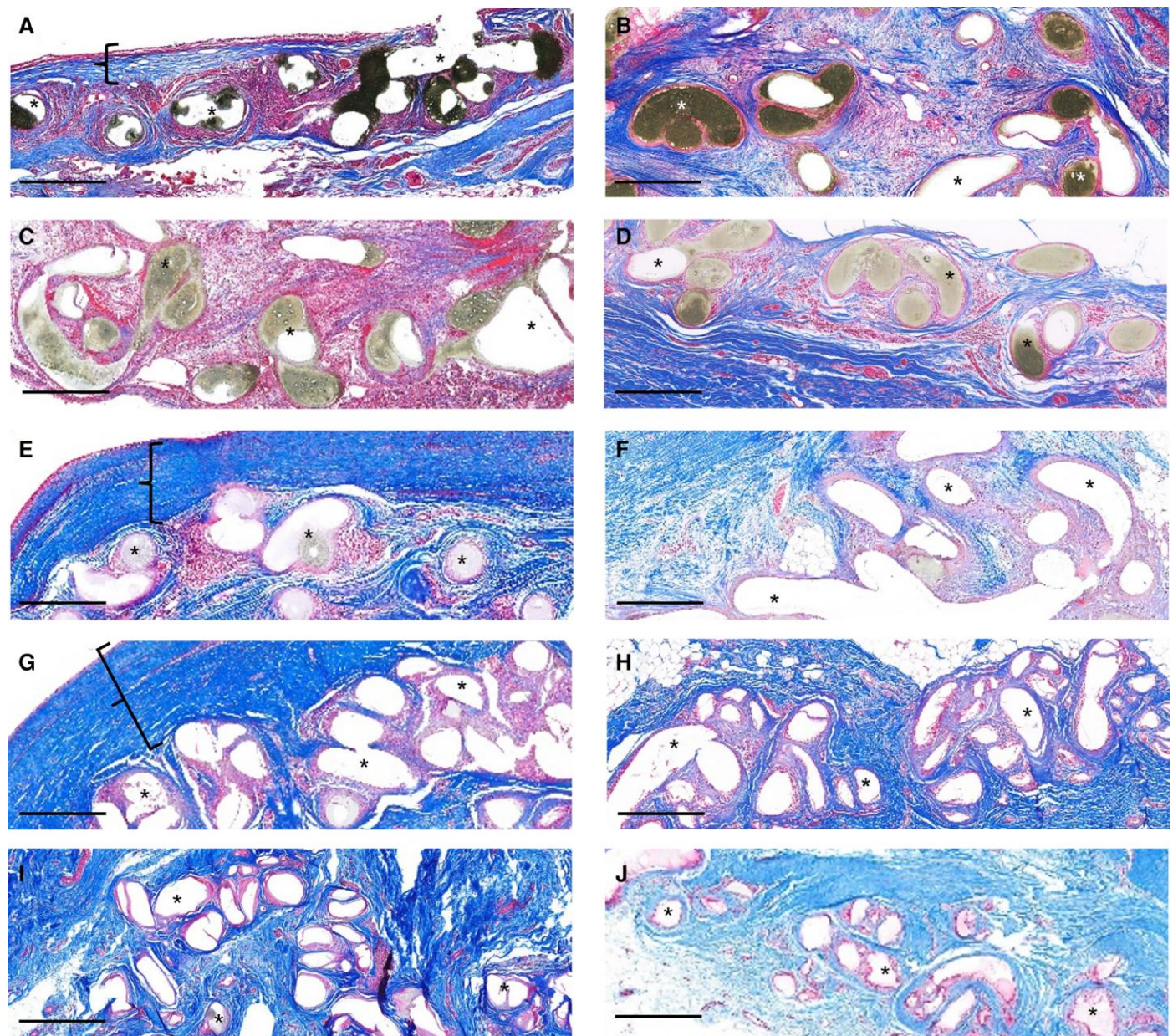


**Figure 2.** Tissue deposition around and within implanted GalaFLEX Scaffolds in the breast tissue. Representative images of Masson's trichrome stained cross sections showing the patterns of collagenous fibrous tissue deposition at 6 weeks (A), 6 months (B), 7 months (C), 9 months (D), 11 months (E), 24 months (F), 27 months (G), 30 months (H), 52 months (I), and 63 months (J) after GalaFLEX Scaffold implantation in the breast. Scale bars 500  $\mu$ m. Asterisks (\*) identify the poly-4-hydroxybutyrate (P4HB) fiber or P4HB remnant material location within the tissue. Left braces (]) indicate an organized band of connective tissue immediately adjacent to the silicone implant location.

fibers. This organized arrangement of fibers was present at all later time points that were represented in the cohort of patients (Figure 2).

It is worth noting that most samples showed randomly distributed small clusters of adipose connective tissue. These adipose clusters were more prominent at earlier time points compared with later time points. The adipose tissue clusters were randomly distributed throughout the thickness of the P4HB scaffold and interspersed within the fibrous connective tissue component.

It is clinically relevant that the spindle-shaped fibroblasts present within the deposited collagen fibers did not stain positive for SMA (Figure 5), the molecular component most responsible for cell and associated tissue contraction. Stated differently, the deposited mature collagen seen in the P4HB specimens was not consistent with the histological presentation seen with the clinical phenomenon of "capsular contraction."<sup>10,24</sup>

## GalaFLEX Scaffolds Support a Vascularized Remodeling Response

The vascularity present within all specimens represented in this study was very robust, consisting of a mixture of capillary-sized vessels and arterioles. The identity of these structures as blood vessels was confirmed by immunolabeling with CD31 (a marker for endothelial cells) (Figure 6) and the presence of an adjacent layer of SMA-positive spindle cells (ie, smooth muscle cells) (Figure 5) that form around arterioles and arteries. There was a modest decrease in the quantity of blood vessels in the specimens that represented longer implant duration, but even these specimens were well vascularized. As connective tissue assumes a more dense and mature phenotype, vascularity typically decreases. This pattern was observed in the present collection of specimens, although as stated above, the amount of

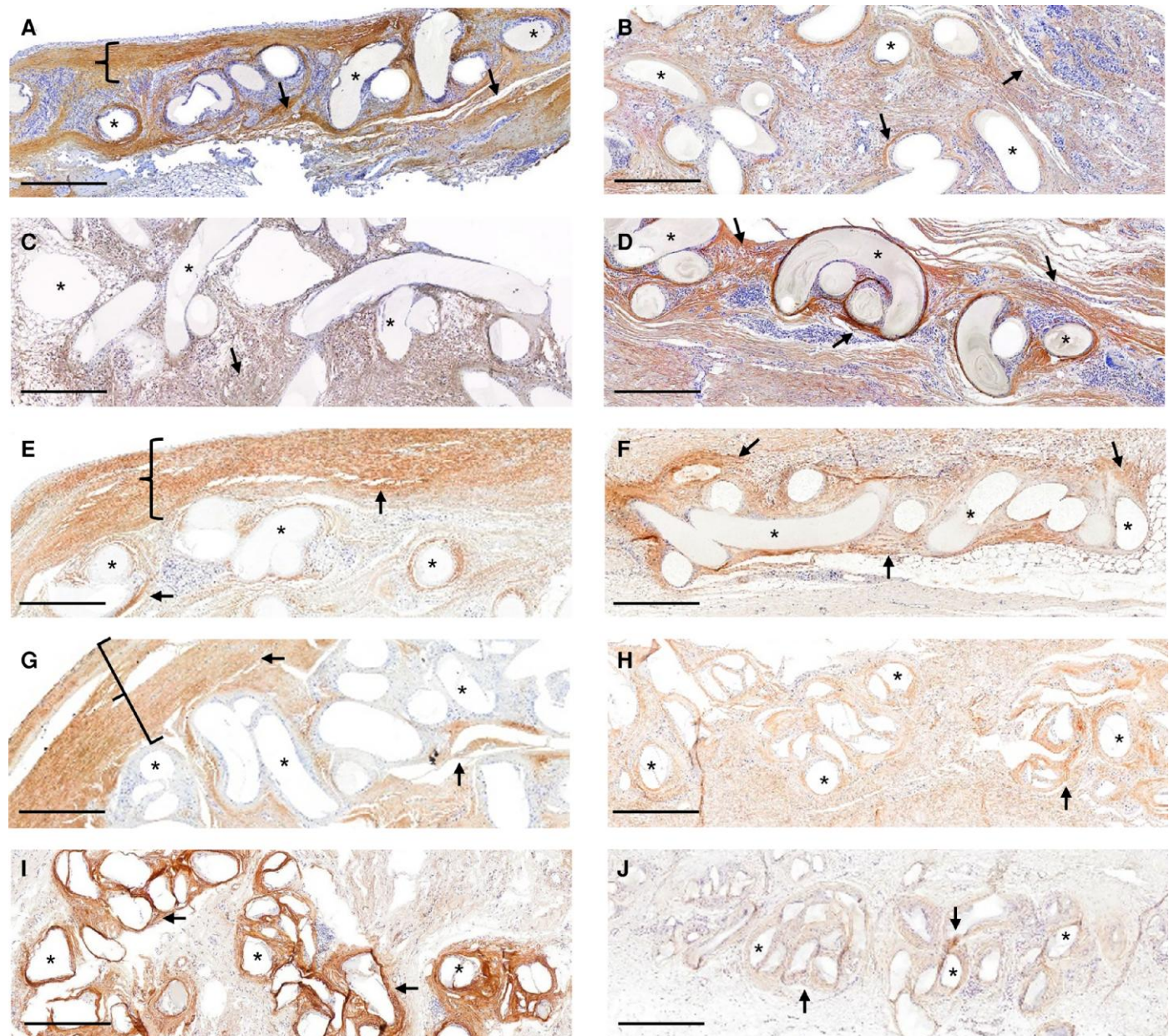


**Figure 3.** Mature collagen Type I around and within implanted GalaFLEX Scaffolds in the breast tissue. Representative images of immunostaining against collagen Type I showing the patterns of mature collagenous fibrous tissue deposition at 6 weeks (A), 6 months (B), 7 months (C), 9 months (D), 11 months (E), 24 months (F), 27 months (G), 30 months (H), 52 months (I), and 63 months (J) after GalaFLEX Scaffold implantation in the breast. Scale bars 500  $\mu$ m. Asterisks (\*) identify the poly-4-hydroxybutyrate (P4HB) fiber or P4HB remnant material location within the tissue. Arrows (→) identify dark brown stain positive for collagen Type I. Left braces ({} ) indicate an organized band of connective tissue immediately adjacent to the silicone implant location.

vascularity was still robust even in the longer implant specimens. Vascularity was less within the scattered islands of adipose tissue, which is consistent with the pattern of vascularity of normal adipose tissue.

## Histomorphologic Interactions of GalaFLEX Scaffolds and Breast Implants

Three of the evaluated specimens were from patients that had an augmentation procedure performed with smooth, round, silicone gel implant (samples from revisions at 6 weeks, 11 and 27 months). The interface between the implant and the GalaFLEX device consisted

of an organized band of collagenous connective tissue with a single layer of epithelioid cells occupying the surface of the fibrous tissue, ie, immediately adjacent to the silicone implant (Figure 1A, E, G).

## DISCUSSION

The use of biologic, biosynthetic, and synthetic scaffolds in breast tissue reinforcement has become commonplace in plastic and reconstructive surgeries.<sup>5,11,25,26</sup> Although not yet FDA-approved for breast augmentation or reconstruction, plastic surgeons often employ these scaffolds off-label, after thoroughly evaluating the associated risks and benefits with patients.<sup>18</sup> These scaffolds

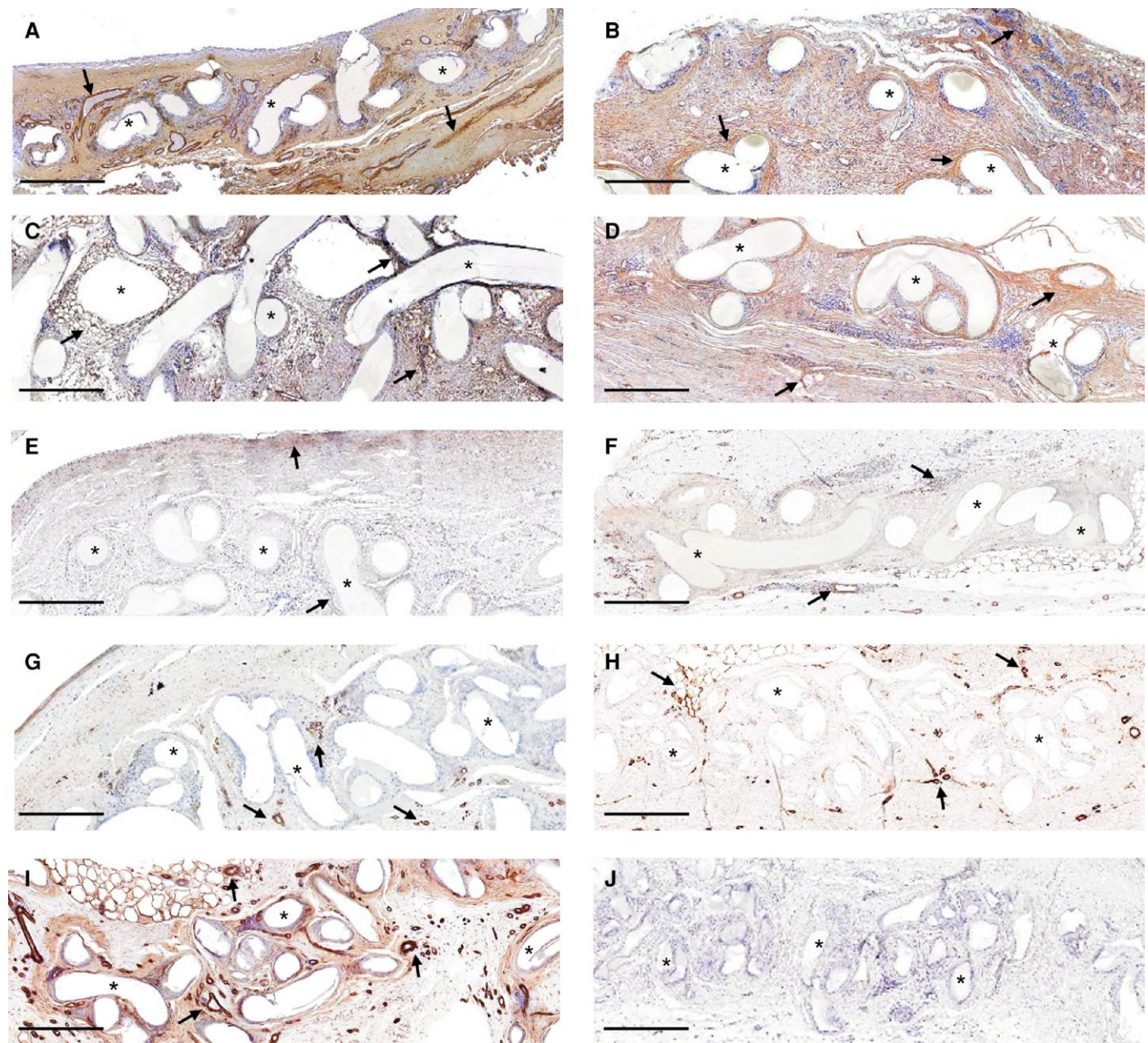


**Figure 4.** Deposition of collagen Type III around implanted GalaFLEX Scaffolds in the breast tissue. Representative images of immunostaining against collagen Type III showing the patterns of new collagenous tissue deposition at 6 weeks (A), 6 months (B), 7 months (C), 9 months (D), 11 months (E), 24 months (F), 27 months (G), 30 months (H), 52 months (I), and 63 months (J) after GalaFLEX Scaffold implantation in the breast. Scale bars 500  $\mu$ m. Asterisks (\*) identify the poly-4-hydroxybutyrate (P4HB) fiber or P4HB remnant material location within the tissue. Arrows (→) identify dark brown stain positive for collagen Type III.

provide structural support to the breast and help improve aesthetic outcomes.<sup>18</sup> Among the commercially available scaffolds, those most commonly used in breast procedures include biologic scaffolds derived from human, porcine, or bovine dermal ECM, such as AlloDerm,<sup>27</sup> Stratattice,<sup>28</sup> FlexHD,<sup>29</sup> and Fortiva;<sup>6,9,10,30</sup> absorbable biosynthetic scaffolds like GalaFLEX<sup>31</sup> Scaffold; and synthetic absorbable scaffolds, such as TIGR Matrix,<sup>32</sup> and DuraSorb<sup>6,10,33</sup> (Table 3).

The specific characteristics of each scaffold, including material composition, 3D structure, and absorption time influence the host immune response and the integration of surrounding breast tissue and associated connective tissues. Previous studies have shown that the GalaFLEX Scaffold provides structural support, long-term retention of breast position, and a reduced rate of capsular contracture when used

for ptosis, whether in combination with breast implants or as a stand-alone soft tissue support.<sup>7,8,11,18</sup> The present study evaluated clinical tissue samples for which GalaFLEX Scaffold was used as a soft tissue support, with and without breast implants, to assess histomorphological integration of the P4HB scaffold over time, from 6 weeks to 63 months, in a cohort of 10 patients that required revision surgery.

The host response to implanted scaffolds is a dynamic process, initiated by blood protein adsorption onto the biomaterial (known as the Vroman effect), and continues until the scaffold is either fully resorbed and eliminated from the host tissue or embedded within the fibrous capsule of the foreign body response.<sup>34</sup> Different phases in this process involve distinct cellular responses that play roles in determining the outcome.<sup>35,36</sup> Following protein adsorption, an acute inflammatory cell response occurs, initially driven by

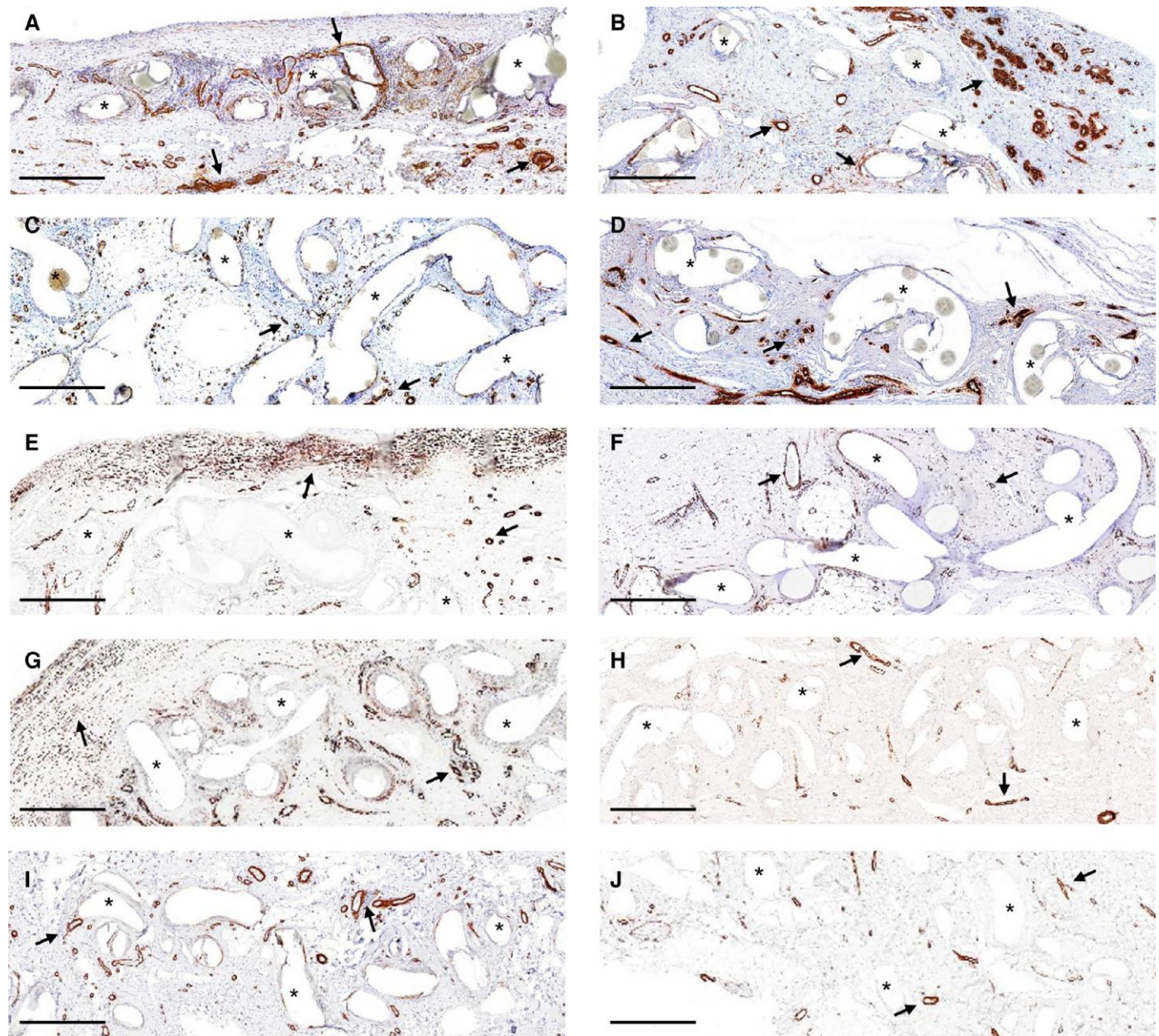


**Figure 5.** Smooth muscle actin (SMA) around implanted GalaFLEX Scaffolds in the breast tissue. Representative images of immunostaining against SMA showing the location of positive vascular myocytes and myofibroblasts at 6 weeks (A), 6 months (B), 7 months (C), 9 months (D), 11 months (E), 24 months (F), 27 months (G), 30 months (H), 52 months (I), and 63 months (J) after GalaFLEX Scaffold implantation in the breast. Scale bars 500  $\mu$ m. Asterisks (\*) identify the poly-4-hydroxybutyrate (P4HB) fiber or P4HB remnant material location within the tissue. Arrows (→) identify dark brown stain positive for SMA.

neutrophils and later by mononuclear cells. This response generates a microenvironment that can either promote a constructive tissue remodeling or lead to chronic inflammation, encapsulation, and fibrosis.<sup>37,38</sup> The activation and plasticity of immune cells, particularly macrophages, during the acute and subacute response (7-14 days post-implantation), influence the eventual outcome. A transition from pro-inflammatory M1-like macrophages to pro-remodeling M2-like macrophages is required to avoid a chronic inflammatory state.<sup>37,39,40</sup>

Histological analysis of the tissue biopsies from the present study showed a dynamic cellular response to the P4HB scaffold. The early timepoints showed the expected acute inflammatory response that progressively transitioned into an active tissue remodeling process. This tissue remodeling was characterized by a non-inflammatory cellular response, neovascularization and deposition of a swarming

pattern of neomatrix. Over time, a steady state was reached in which spindle cells and a low number of mononuclear cells comprised the microenvironment surrounding the remaining fiber architecture. This steady state with the presence of identifiable P4HB fiber substance persisted for at least 63 months.

The *in vivo* degradation of P4HB primarily occurs through bulk hydrolysis of the polymer with degradation product consisting of the 4HB monomer or oligomer, a short-chain naturally occurring fatty acid that is found in various tissues of the body.<sup>12,16</sup> Prior studies have shown that 4HB can activate molecular pathways in macrophages that promote the secretion of antimicrobial peptides, helping protect the tissue from bacterial infection.<sup>16,41</sup> Ultimately, 4HB is metabolized through the Krebs cycle, with carbon dioxide ( $\text{CO}_2$ ) and water ( $\text{H}_2\text{O}$ ) as the final byproducts, without accumulating any harmful secondary metabolites.<sup>12</sup>

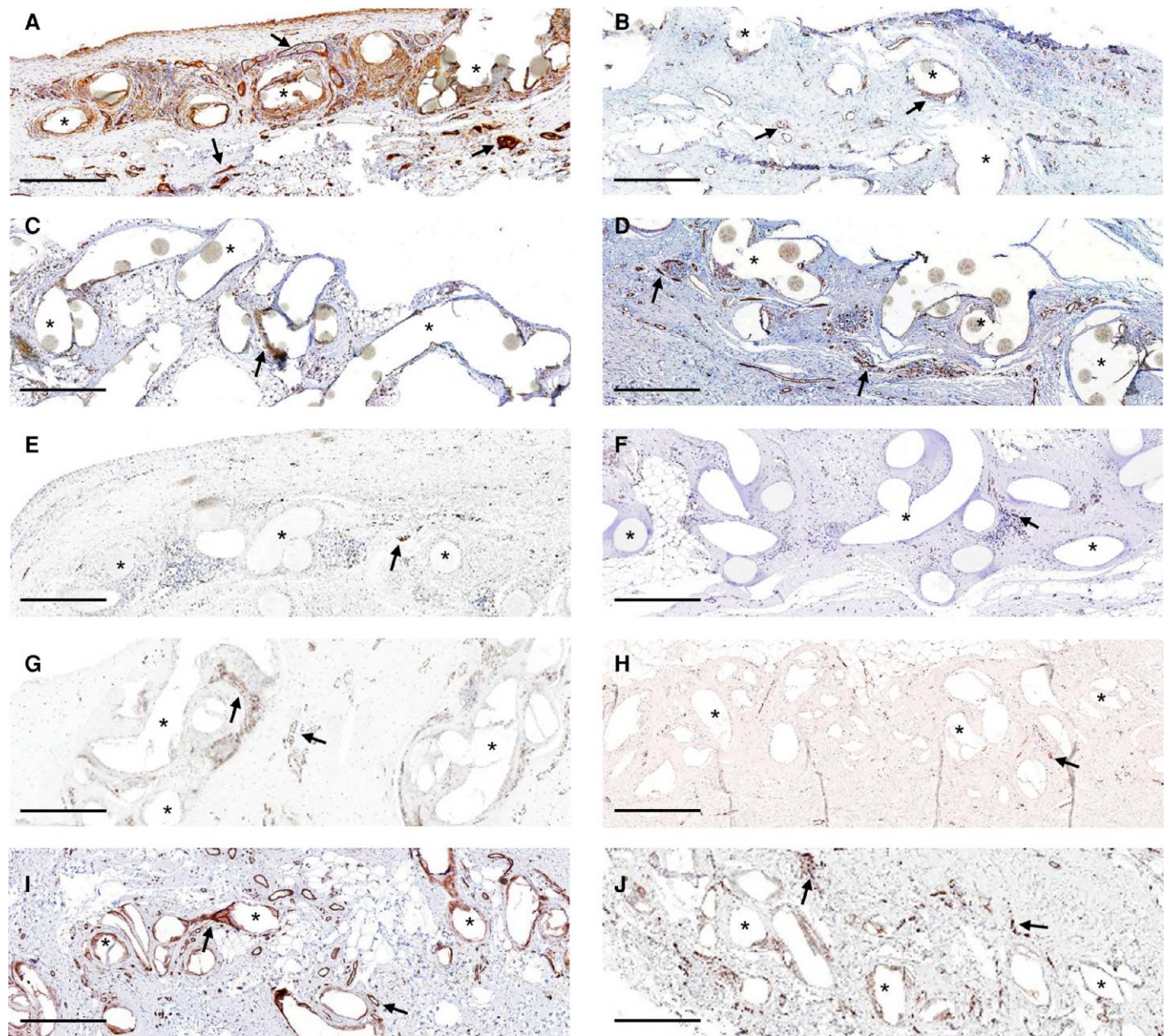


**Figure 6.** Vascularization around implanted GalaFLEX Scaffolds in the breast tissue. Representative images of immunostaining against DC-31 showing blood vessels around and within the GalaFLEX Scaffold at 6 weeks (A), 6 months (B), 7 months (C), 9 months (D), 11 months (E), 24 months (F), 27 months (G), 30 months (H), 52 months (I), and 63 months (J) after implantation in the breast. Scale bars 500  $\mu$ m. Asterisks (\*) identify the poly-4-hydroxybutyrate (P4HB) fiber or P4HB remnant material location within the tissue. Arrows (→) identify dark brown stain positive for DC-31.

This degradation profile is consistent with previous reports on P4HB meshes in both animal models and clinical applications.<sup>20,42</sup> As the P4HB mass decreases over time, the mechanical strength of the scaffold diminishes after ~12 to 18 months.<sup>42</sup>

Collagen deposition is an important aspect of tissue remodeling, including applications involving the breast. Such collagen deposition occurs largely in response to mechanical forces.<sup>43,44</sup> The organization and density of collagen observed in the tissue specimens followed Davis's law, which states that the amount and organization of connective tissue deposition is a direct and appropriate consequence of the applied forces.<sup>45</sup> In the present cohort of patients, the applied forces consisted of the weight and pressure from adjacent tissues and associated implants. The collagen and ECM components that were deposited within and around the GalaFLEX Scaffold showed tissue integration, not

encapsulation. Encapsulation would typically result in a band of connective tissue around the exterior of the entire scaffold, without extending into the interfiber spaces. The pattern of collagen deposition with vascularization observed over the course of 6 weeks to 63 months was consistent with a constructive tissue remodeling response.

Tissue vascularization is crucial for the homeostasis of the tissue, providing oxygen, nutrients, and defense mechanisms against infections.<sup>46</sup> In the case of implanted scaffolds, a robust blood supply is even more critical as it supports cellular infiltration, new tissue deposition, and protection against infection. As cells infiltrate the scaffold through the porous structure, they require an oxygen supply that is derived from diffusion of  $O_2$  from adjacent blood vessels.<sup>47</sup> All examined tissue specimens, from 6 weeks to 63 months, exhibited a robust vascularization, indicating a supportive microenvironment within the scaffold. Since all

**Table 3.** Composition and Properties of Scaffold Materials Used in Breast Plastic and Reconstructive Surgery

Commercial scaffold name	Composition	Category	In vivo resorption time	Ref.
AlloDerm	Human-derived acellular dermal matrix	Biologic scaffold	12 Months	<a href="#">27</a>
Strattice	Porcine-derived acellular dermal matrix	Biologic scaffold	12 Months	<a href="#">28</a>
FlexHD	Human-derived acellular dermal matrix	Biologic scaffold	12 Months	<a href="#">29</a>
Fortiva	Porcine-derived acellular dermal matrix	Biologic scaffold	12 Months	<a href="#">30</a>
GalaFLEX	Poly 4-hydroxybutyrate (P4HB)	Biosynthetic absorbable monofilament	12-18 Months	<a href="#">31</a>
TIGR	Fast resorbing copolymer: glycolide, lactide and trimethylene carbonate (TMC) Slow resorbing copolymer: lactide and trimethylene carbonate	Synthetic absorbable multifilament	4 and 26 Months	<a href="#">32</a>
DuraSorb	Poly dioxanone	Synthetic absorbable monofilament	9 Months	<a href="#">33</a>

Ref, reference.

biomedical implants are at risk for contamination/infection, the vascularity present in these samples provides assurance that the host immune system is fully available to minimize the risk of scaffold infection. A rich vascular supply is capable of supporting a constructive connective tissue remodeling response and necessary for sustained functionality.

There are limitations to the present study. Biopsy specimens were collected from 10 patients, a relatively small number without biologic replicates of the evaluated timepoints. Larger cohort studies, especially those including a diverse patient population, are warranted in future studies to validate the results of this study.

## CONCLUSIONS

This study provides valuable insights into the histomorphologic characteristics of tissue integration and the long-term degradation profile of the GalaFLEX Scaffold in breast tissue. The slow degradation of the scaffold, the patterns of tissue remodeling around and within the fibers, and the ability to support vascularization at the interfiber spaces demonstrate its potential as a safe and effective adjunct in breast plastic and reconstructive surgery.

## Acknowledgments

Drs Van Natta and Pineda Molina made an equal contribution to this work as co-first authors. The authors would like to acknowledge Alizée Pathology, LLC, Serge D. Rousselle, Molly Friedemann, and James R. L. Stanley for their assistance.

## Disclosures

Drs Van Natta, Pineda Molina, Hussey, and Badylak are consultants with Becton Dickinson and Co. (BD, Franklin Lakes, NJ). Dr Van Natta is the past president of The Aesthetic Foundation (Garden Grove, CA). Dr Antonelli declared no potential conflicts of interest with respect to the research, authorship, and publication of this article.

## Funding

The University of Pittsburgh (Pittsburgh, PA) holds a Physician-Scientist Institutional Award from the Burroughs Wellcome Fund (Vincent Antonelli). Research reported in this

publication was supported by the National Cancer Institute at the National Institutes of Health (Bethesda, MD, USA) under award number T32CA113263 (Vincent Antonelli).

## REFERENCES

1. Liu L, Kim L, Teotia SS, Haddock NT. Long-term implications of cosmetic breast surgeries on subsequent breast reconstruction. *Aesthet Surg J.* 2024;44:1300-1308. doi: [10.1093/asj/sjae138](https://doi.org/10.1093/asj/sjae138)
2. Aesthetic plastic surgery national databank statistics 2022. *Aesthet Surg J.* 2023;43:1-19. doi: [10.1093/asj/sjad354](https://doi.org/10.1093/asj/sjad354)
3. American Society of Plastic Surgeons. 2023 Plastic surgery statistics report. 2024. Accessed November 14, 2024. <https://www.plasticsurgery.org/news/plastic-surgery-statistics>
4. Albornoz CR, Bach PB, Mehrara BJ, et al. A paradigm shift in U.S. Breast reconstruction: increasing implant rates. *Plast Reconstr Surg.* 2013;131:15-23. doi: [10.1097/PRS.0b013e3182729cde](https://doi.org/10.1097/PRS.0b013e3182729cde)
5. Tomouk T, Georgeu G. Use of a biological scaffold in the cleavage area in complex revision breast augmentation: a surgical technique and case series. *J Plast Reconstr Aesthet Surg.* 2023;78:75-81. doi: [10.1016/j.bjps.2023.01.031](https://doi.org/10.1016/j.bjps.2023.01.031)
6. Hu Y, Diao W, Wen S, et al. The usage of mesh and relevant prognosis in implant breast reconstruction surgery: a meta-analysis. *Aesthetic Plast Surg.* 2024;48:3386-3399. doi: [10.1007/s00266-024-03879-5](https://doi.org/10.1007/s00266-024-03879-5)
7. Mallucci P, Bistoni G. Experience and indications for the use of the P4HB scaffold (GalaFLEX) in aesthetic breast surgery: a 100-case experience. *Aesthet Surg J.* 2022;42:1394-1405. doi: [10.1093/asj/sjac198](https://doi.org/10.1093/asj/sjac198)
8. Bucceri EM, Villanucci A, Mallucci P, Bistoni G, de Vita R. Synthetic reabsorbable mesh (GalaFLEX) as soft tissue adjunct in breast augmentation revision surgery. *Aesthet Surg J.* 2023;43:559-566. doi: [10.1093/asj/sjac326](https://doi.org/10.1093/asj/sjac326)
9. Durando M, Ferrando PM, Dianzani C, et al. Acellular dermal matrix imaging features in breast reconstructive surgery: a pictorial review. *Br J Radiol.* 2024;97:505-512. doi: [10.1093/bjr/tqad050](https://doi.org/10.1093/bjr/tqad050)
10. Bai J, Ferenz S, Fracol M, Kim JY. Revision breast reconstruction with biologic or synthetic mesh: an analysis of postoperative capsular contracture rates. *Aesthet Surg J Open Forum.* 2024;6:ojae035. doi: [10.1093/asjof/ojae035](https://doi.org/10.1093/asjof/ojae035)
11. Nair NM, Mills DC. Poly-4-hydroxybutyrate (P4HB) scaffold internal support: preliminary experience with direct implant opposition during complex breast revisions. *Aesthet Surg J.* 2019;39:1203-1213. doi: [10.1093/asj/sjy276](https://doi.org/10.1093/asj/sjy276)
12. Williams SF, Rizk S, Martin DP. Poly-4-hydroxybutyrate (P4HB): a new generation of resorbable medical devices for tissue repair and regeneration. *Biomed Tech (Berl).* 2013;58:439-452. doi: [10.1515/bmt-2013-0009](https://doi.org/10.1515/bmt-2013-0009)
13. Buell JF, Sigmor D, Ducoin C, et al. Initial experience with biologic polymer scaffold (poly-4-hydroxybutyrate) in complex abdominal wall reconstruction. *Ann Surg.* 2017;266:185-188. doi: [10.1097/SLA.0000000000001916](https://doi.org/10.1097/SLA.0000000000001916)
14. Plymale MA, Davenport DL, Dugan A, Zachem A, Roth JS. Ventral hernia repair with poly-4-hydroxybutyrate mesh. *Surg Endosc.* 2018;32:1689-1694. doi: [10.1007/s00464-017-5848-7](https://doi.org/10.1007/s00464-017-5848-7)

15. Pineda Molina C, Giglio R, Gandhi RM, et al. Comparison of the host macrophage response to synthetic and biologic surgical meshes used for ventral hernia repair. *J Immunol Regen Med.* 2019;3:13-25. doi: [10.1016/j.regen.2018.12.002](https://doi.org/10.1016/j.regen.2018.12.002)

16. Pineda Molina C, Hussey GS, Eriksson J, et al. 4-Hydroxybutyrate promotes endogenous antimicrobial peptide expression in macrophages. *Tissue Eng Part A.* 2019;25:693-706. doi: [10.1089/ten.TEA.2018.0377](https://doi.org/10.1089/ten.TEA.2018.0377)

17. Karp N, Sorenson TJ, Boyd CJ, et al. The GalaFLEX 'empanada' for direct to implant prepectoral breast reconstruction. *Plast Reconstr Surg.* 2024;155: 488e-491e. doi: [10.1097/PRS.00000000000011592](https://doi.org/10.1097/PRS.00000000000011592)

18. Movassagh K, Gilson A, Stewart CN, Cusic J, Movassagh A. Prepectoral two-stage implant-based breast reconstruction with poly-4-hydroxybutyrate for pocket control without the use of acellular dermal matrix: a 4-year review. *Plast Reconstr Surg.* 2024;154:15-24. doi: [10.1097/PRS.00000000000010914](https://doi.org/10.1097/PRS.00000000000010914)

19. Adams WP Jr, Baxter R, Glicksman C, Mast BA, Tantillo M, Van Natta BW. The use of poly-4-hydroxybutyrate (P4HB) scaffold in the ptotic breast: a multicenter clinical study. *Aesthet Surg J.* 2018;38:502-518. doi: [10.1093/asj/sjy022](https://doi.org/10.1093/asj/sjy022)

20. Rehne RD, Clarke JM, Goodrum AJ, Badylak SF. Absorbable biosynthetic scaffolds in place of silicone for breast reconstruction: a 9-year experience with 53 patients. *Plast Reconstr Surg Glob Open.* 2024;12:e5821. doi: [10.1097/GOX.0000000000005821](https://doi.org/10.1097/GOX.0000000000005821)

21. Zierle-Ghosh A, Jan A. *Physiology, Body Mass Index.* StatPearls; 2023.

22. Wynn TA, Vannella KM. Macrophages in tissue repair, regeneration, and fibrosis. *Immunity.* 2016;44:450-462. doi: [10.1016/j.immuni.2016.02.015](https://doi.org/10.1016/j.immuni.2016.02.015)

23. Zhang X, Kang X, Jin L, Bai J, Liu W, Wang Z. Stimulation of wound healing using bioinspired hydrogels with basic fibroblast growth factor (bFGF). *Int J Nanomedicine.* 2018;13:3897-3906. doi: [10.2147/IJN.S168998](https://doi.org/10.2147/IJN.S168998)

24. Larsen A, Timmermann AM, Kring M, et al. A histological assessment tool for breast implant capsules validated in 480 patients with and without capsular contracture. *Aesthetic Plast Surg.* 2024;49:497-508. doi: [10.1007/s00266-024-04128-5](https://doi.org/10.1007/s00266-024-04128-5)

25. Wallace L, Wokes JET. Internal bra: a literature review and sub-classification of definitions. *Aesthetic Plast Surg.* 2024;48:3298-3303. doi: [10.1007/s00266-023-03802-4](https://doi.org/10.1007/s00266-023-03802-4)

26. Wazir U, Patani N, Heeney J, Mokbel K, Mokbel K. Pre-pectoral immediate breast reconstruction following conservative mastectomy using acellular dermal matrix and semi-smooth implants. *Anticancer Res.* 2022;42:1013-1018. doi: [10.21873/anticanres.15562](https://doi.org/10.21873/anticanres.15562)

27. Cole PD, Stal D, Sharabi SE, Hicks J, Hollier LH Jr. A comparative, long-term assessment of four soft tissue substitutes. *Aesthet Surg J.* 2011;31:674-681. doi: [10.1177/1090820X11415393](https://doi.org/10.1177/1090820X11415393)

28. Cavallo JA, Greco SC, Liu J, Frisella MM, Deeken CR, Matthews BD. Remodeling characteristics and biomechanical properties of a crosslinked versus a non-crosslinked porcine dermis scaffolds in a porcine model of ventral hernia repair. *Hernia.* 2015;19:207-218. doi: [10.1007/s10029-013-1070-2](https://doi.org/10.1007/s10029-013-1070-2)

29. Tork S, Jefferson RC, Janis JE. Acellular dermal matrices: applications in plastic surgery. *Semin Plast Surg.* 2019;33:173-184. doi: [10.1055/s-0039-1693019](https://doi.org/10.1055/s-0039-1693019)

30. Kockerling F, Alam NN, Antoniou SA, et al. What is the evidence for the use of biologic or biosynthetic meshes in abdominal wall reconstruction? *Hernia.* 2018;22:249-269. doi: [10.1007/s10029-018-1735-y](https://doi.org/10.1007/s10029-018-1735-y)

31. Martin DP, Badhwar A, Shah DV, et al. Characterization of poly-4-hydroxybutyrate mesh for hernia repair applications. *J Surg Res.* 2013;184: 766-773. doi: [10.1016/j.jss.2013.03.044](https://doi.org/10.1016/j.jss.2013.03.044)

32. Deeken CR, Abdo MS, Frisella MM, Matthews BD. Physicomechanical evaluation of polypropylene, polyester, and polytetrafluoroethylene meshes for inguinal hernia repair. *J Am Coll Surg.* 2011;212:68-79. doi: [10.1016/j.jamcollsurg.2010.09.012](https://doi.org/10.1016/j.jamcollsurg.2010.09.012)

33. Mlodinow AS, Yerneni K, Hasse ME, Cruikshank T, Kuzycz MJ, Ellis MF. Evaluation of a novel absorbable mesh in a porcine model of abdominal wall repair. *Plast Reconstr Surg Glob Open.* 2021;9:e3529. doi: [10.1097/GOX.0000000000003529](https://doi.org/10.1097/GOX.0000000000003529)

34. Londono R, Badylak SF. Chapter 1: factors which affect the host response to biomaterials. In: Badylak SF, ed. *Host Response to Biomaterials the Impact of Host Response on Biomaterial Selection.* Elsevier; 2015:1-10.

35. Young A, McNaught C-E. The physiology of wound healing. *Surgery (Oxford).* 2011;29:475-479. doi: [10.1016/j.mpsur.2011.06.011](https://doi.org/10.1016/j.mpsur.2011.06.011)

36. Witte MB, Barbul A. General principles of wound healing. *Surg Clin North Am.* 1997;77:509-528. doi: [10.1016/s0039-6109\(05\)70566-1](https://doi.org/10.1016/s0039-6109(05)70566-1)

37. Brown BN, Londono R, Tottey S, et al. Macrophage phenotype as a predictor of constructive remodeling following the implantation of biologically derived surgical mesh materials. *Acta Biomater.* 2012;8:978-987. doi: [10.1016/j.actbio.2011.11.031](https://doi.org/10.1016/j.actbio.2011.11.031)

38. Brown BN, Sicari BM, Badylak SF. Rethinking regenerative medicine: a macrophage-centered approach. *Front Immunol.* 2014;5:510. doi: [10.3389/fimmu.2014.00510](https://doi.org/10.3389/fimmu.2014.00510)

39. Wolf MT, Carruthers CA, Dearth CL, et al. Polypropylene surgical mesh coated with extracellular matrix mitigates the host foreign body response. *J Biomed Mater Res A.* 2014;102:234-246. doi: [10.1002/jbm.a.34671](https://doi.org/10.1002/jbm.a.34671)

40. Wolf MT, Vodovotz Y, Tottey S, Brown BN, Badylak SF. Predicting in vivo responses to biomaterials via combined in vitro and in silico analysis. *Tissue Eng Part C Methods.* 2015;21:148-159. doi: [10.1089/ten.TEC.2014.0167](https://doi.org/10.1089/ten.TEC.2014.0167)

41. Pineda Molina C, Hussey GS, Liu A, Eriksson J, D'Angelo WA, Badylak SF. Role of 4-hydroxybutyrate in increased resistance to surgical site infections associated with surgical meshes. *Biomaterials.* 2021;267:120493. doi: [10.1016/j.biomaterials.2020.120493](https://doi.org/10.1016/j.biomaterials.2020.120493)

42. Deeken CR, Matthews BD. Characterization of the mechanical strength, resorption properties, and histologic characteristics of a fully absorbable material (poly-4-hydroxybutyrate-PHASIX mesh) in a porcine model of hernia repair. *ISRN Surg.* 2013;2013:238067. doi: [10.1155/2013/238067](https://doi.org/10.1155/2013/238067)

43. Eichinger JF, Haeusel LJ, Paukner D, Aydin RC, Humphrey JD, Cyron CJ. Mechanical homeostasis in tissue equivalents: a review. *Biomech Model Mechanobiol.* 2021;20:833-850. doi: [10.1007/s10237-021-01433-9](https://doi.org/10.1007/s10237-021-01433-9)

44. Humphrey JD, Dufresne ER, Schwartz MA. Mechanotransduction and extracellular matrix homeostasis. *Nat Rev Mol Cell Biol.* 2014;15:802-812. doi: [10.1038/nrm3896](https://doi.org/10.1038/nrm3896)

45. Cyron CJ, Humphrey JD. Growth and remodeling of load-bearing biological soft tissues. *Meccanica.* 2017;52:645-664. doi: [10.1007/s11012-016-0472-5](https://doi.org/10.1007/s11012-016-0472-5)

46. Humphrey JD, Schwartz MA. Vascular mechanobiology: homeostasis, adaptation, and disease. *Annu Rev Biomed Eng.* 2021;23:1-27. doi: [10.1146/annurev-bioeng-092419-060810](https://doi.org/10.1146/annurev-bioeng-092419-060810)

47. Yang G, Mahadik B, Choi JY, Fisher JP. Vascularization in tissue engineering: fundamentals and state-of-art. *Prog Biomed Eng.* 2020;2:012002. doi: [10.1088/2516-1091/ab5637](https://doi.org/10.1088/2516-1091/ab5637)